LETTERS

Parvalbumin neurons and gamma rhythms enhance cortical circuit performance

Vikaas S. Sohal[1]*, Feng Zhang[1]*, Ofer Yizhar[1] & Karl Deisseroth[1]

Synchronized oscillations and inhibitory interneurons have important and interconnected roles within cortical microcircuits. In particular, interneurons defined by the fast-spiking phenotype and expression of the calcium-binding protein parvalbumin[1,2] have been suggested to be involved in gamma (30–80 Hz) oscillations[3–7], which are hypothesized to enhance information processing[8,9]. However, because parvalbumin interneurons cannot be selectively controlled, definitive tests of their functional significance in gamma oscillations, and quantitative assessment of the impact of parvalbumin interneurons and gamma oscillations on cortical circuits, have been lacking despite potentially enormous significance (for example, abnormalities in parvalbumin interneurons may underlie altered gamma-frequency synchronization and cognition in schizophrenia[10] and autism[11]). Here we use a panel of optogenetic technologies[12–14] in mice to selectively modulate multiple distinct circuit elements in neocortex, alone or in combination. We find that inhibiting parvalbumin interneurons suppresses gamma oscillations *in vivo*, whereas driving these interneurons (even by means of non-rhythmic principal cell activity) is sufficient to generate emergent gamma-frequency rhythmicity. Moreover, gamma-frequency modulation of excitatory input in turn was found to enhance signal transmission in neocortex by reducing circuit noise and amplifying circuit signals, including inputs to parvalbumin interneurons. As demonstrated here, optogenetics opens the door to a new kind of informational analysis of brain function, permitting quantitative delineation of the functional significance of individual elements in the emergent operation and function of intact neural circuitry.

We first developed a versatile system to selectively express microbial opsins, enhanced *Natronomonas pharaonis* halorhodopsin (eNpHR) or channelrhodopsin-2 (ChR2), in fast-spiking parvalbumin (PV) interneurons. Although opsin expression can be targeted with a PV promoter fragment[15], the resulting level of expression was insufficient to drive action potentials reliably (data not shown). We therefore devised (Supplementary Information) a Cre-recombinase-dependent adeno-associated virus (AAV) expression system carrying a reversed[16] and doubled-floxed transgene to enable selective expression in transgenic mice expressing Cre recombinase under the control of the PV promoter (*PV*::*Cre*). This approach decouples transcriptional strength from the specificity of the PV promoter, allowing expression of microbial opsins driven by the strong *EF1α* promoter (Supplementary Information). We found leak to be undetectable and the opsin expression level to be robust (Supplementary Fig. 1a–c), indicating the quantitative suitability of this strategy for probing the causal role of these neurons in neocortical processing.

Cre-dependent *eNpHR–eYFP* (enhanced yellow fluorescent protein) or *ChR2–eYFP* AAV5 vectors were stereotactically injected into the cortex of *PV*::*Cre* transgenic mice. Numerous interneurons with eYFP fluorescence were observed (Fig. 1c, left); in contrast, injection of this construct into wild-type mice revealed no detectable expression (Fig. 1c, right panels), indicating specificity to PV interneurons. Although PV co-staining is less reliable (PV expression in fast-spiking cells can drop below the staining detection limit[17]), immunohistochemistry also revealed both co-localization of eYFP-tagged microbial opsins with PV immunoreactive cells and successful transduction of a substantial fraction of PV cells (Supplementary Fig. 1d; note that the PV interneuron population is heterogenous and not all PV interneurons necessarily express Cre in a given line). As anticipated from the robust expression achieved with the double-floxed strategy, cells expressing either eNpHR–eYFP or ChR2–eYFP displayed strong photocurrents (Supplementary Fig. 1e, f). In particular, in PV interneurons expressing eNpHR–eYFP, yellow light elicited hyperpolarizing currents that inhibited spiking (Fig. 1d, e).

We used this system to test whether PV interneuron activity could be involved in gamma oscillation generation *in vivo*. We injected *Camk2α* (*CaMKIIα*)::*ChR2–eYFP* and Cre-dependent *eNpHR–eYFP* AAV5 into the prefrontal cortex of *PV*::*Cre* transgenic mice, yielding simultaneous ChR2 expression in pyramidal (PY) neurons and eNpHR expression in fast-spiking PV interneurons (Fig. 1f). Local field potentials *in vivo* (Fig. 1g) revealed that single flashes of blue light delivered in naturalistic trains were followed by gamma oscillations (Fig. 1h–j) that were strongly phase-locked to flashes (Fig. 1k); evoked activity was largely limited to the gamma band. We used wavelet methods (Supplementary Information) to measure power at various frequencies after blue flashes, and found that yellow light suppressed gamma power (Fig. 1h, l; 20 ± 4%, mean ± s.e.m.), but did not reduce non-gamma power ($P < 0.001$; recordings from 4 different locations in 2 mice; inhibition is in the range expected from the observations that ~41% of PV interneurons express eNpHR under these conditions and that yellow light suppresses ~65% of PV spikes).

Because inhibition of PV interneurons was found to suppress gamma power, we next sought to determine whether stimulating PV cells could elicit gamma oscillations in downstream PY neurons. To achieve precise and specific control of inputs to PV and PY neurons, we used brain slices from *PV*::*Cre* mice injected with Cre-dependent *ChR2–eYFP* AAV5 in prefrontal cortex. Blue light drove spikes in PV interneurons and inhibited spikes in PY cells, as expected (Fig. 2a, b), in a $GABA_A$ (γ-aminobutyric acid subtype A)-receptor-dependent manner (blocked by 50 μM picrotoxin; data not shown). Next we used dynamic-clamp technique to inject well-defined trains of simulated excitatory post-synaptic currents (sEPSCs) into PY neurons, and drove fast-spiking PV interneurons by delivering light flashes triggered by observed PY neuron spikes, thereby implementing classical feedback inhibition (Fig. 2c; the delay between spike detection and onset of inhibitory post-synaptic responses was

[1]Department of Bioengineering, Department of Psychiatry and Behavioral Sciences, W083 Clark Center, 318 Campus Drive West, Stanford University, Stanford, California 94305, USA.
*These authors contributed equally to this work.

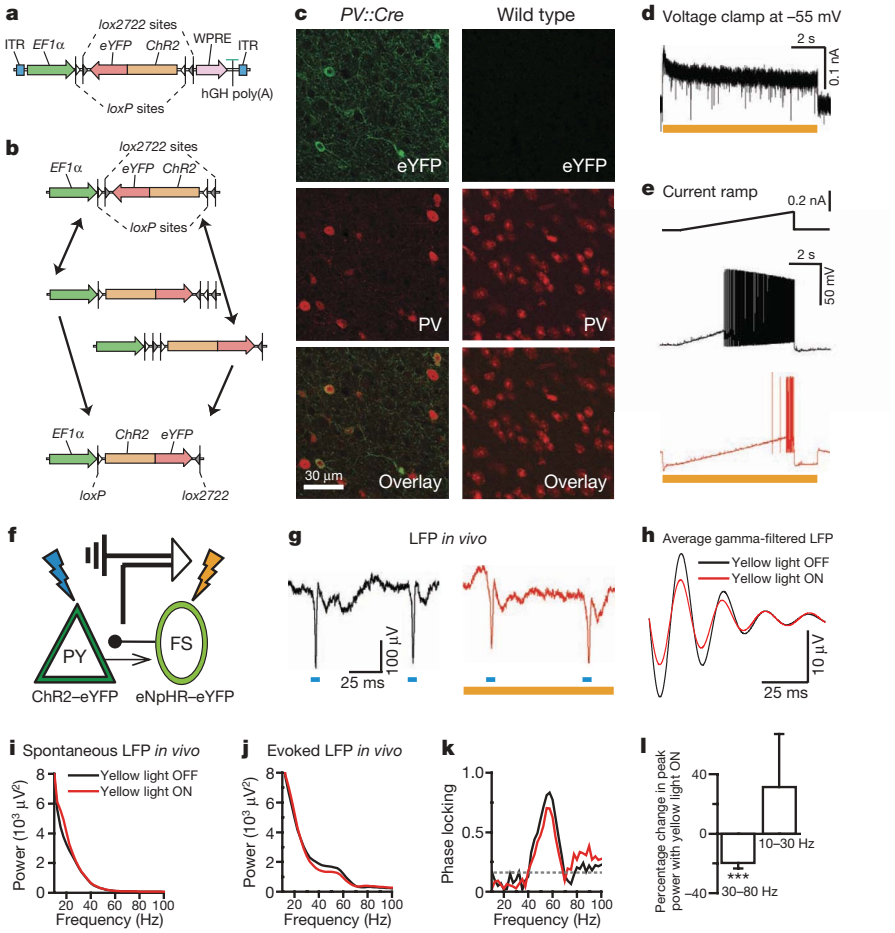

Figure 1 | Inhibiting PV cells suppresses gamma oscillations *in vivo*. **a**, Double-floxed Cre-dependent AAV vector design. hGH, human growth hormone polyadenylation signal; ITR, inverted terminal repeat; WPRE, woodchuck heptatitis virus post-transcriptional regulatory element. **b**, Recombination pathways to low-leak Cre-dependent expression. **c**, Left: antibody-stained PV cells (red) expressing ChR2–eYFP (green) in prefrontal cortex (PFC) of *PV*::*Cre* mice after injection of Cre-dependent AAV. Right: absent ChR2–eYFP expression in similarly treated wild-type mice. **d**, Yellow-light-evoked outward current in eNpHR-expressing PV cells in acute slice. **e**, Effect of yellow light on current-ramp-evoked spiking in the same cell. **f**, Experimental design: *in vivo* local field potentials (LFPs) recorded in mouse PFC; blue and yellow light modulate ChR2(+) PY and eNpHR(+) fast-spiking (FS)/PV cells, respectively. **g**, Sample blue-light-evoked LFPs; **g**–**k** show data from a single location *in vivo*; red traces denote recordings in yellow light. **h**, Filtered (35–45 Hz)-light-evoked LFPs. **i**, Spontaneous LFP power spectra. **j**, Blue-light-evoked LFP power spectra. **k**, Yellow light modulation of phase-locking (Supplementary Information). Dotted line denotes statistical significance. **l**, Effect of fast-spiking cell inhibition on peak power at gamma and lower frequencies ($n = 4$ recording locations; $^{***}P < 0.001$). Error bars, mean and s.e.m.

~3 ms and light is predicted to drive ~2–4 PV interneurons per field; Supplementary Information). Notably, during responses to entirely non-rhythmic sEPSC trains (Fig. 2d), PV interneuron-mediated feedback inhibition by itself markedly enhanced power in the gamma range, but not at other frequencies (representative cell in Fig. 2e; population data in Fig. 2f; $n = 4$ cells, $P < 0.05$ by two-tailed t-test here and in other figures). Quantitatively comparable levels of feedback inhibition delivered with dynamic clamp to PY cells rather than with PV interneuron stimulation were not effective at enhancing gamma power ($n = 4$ cells; Supplementary Tables 1 and 2), pointing to a specialized role of PV interneurons in generating emergent gamma oscillations within neocortical microcircuits.

We next sought to quantify effects of gamma oscillations on information processing. We used dynamic-clamp technique to drive PY neurons ($n = 14$) with precisely defined trains of sEPSCs (Fig. 3a). During each train, the rate of input sEPSCs was varied from 0 Hz to 500 Hz; to create rhythmic inputs, each sEPSC train was further modulated by means of 25-ms cycles (40 Hz; gamma) or 125-ms cycles (8 Hz; theta)[18,19]. For each condition, we measured output spike rate as a function of input sEPSC rate (representative neuron in Fig. 3b). In all conditions, mean spike rate increased with sEPSC rate, and gamma (but not theta) oscillations increased the gain—that is, the maximal slope—of the neuronal input–output curve (Fig. 3c; $P < 0.001$, $n = 14$ cells). Both gamma and theta modulation also significantly reduced response variability (mean normalized standard deviation of responses to each input sEPSC rate; Supplementary Information; Fig. 3d; $P < 0.001$). Detailed quantification of the effect of rhythmic modulation requires informational measures, because it is otherwise not clear whether (for example) steepening of the input–output curve for input rates near 200 Hz, or flattening of the curve near 400 Hz, has a greater impact on information transmission properties.

Mutual information[20] can quantify the information a neural output carries about an input signal, defined as the difference between response entropy (variability of output) and noise entropy (how much output variability is unrelated to input; Supplementary Information). Both theta and gamma modulation markedly increased mutual information between input sEPSC rate and output spike rate (Fig. 3e). In particular, gamma modulation increased the amount of information that spike rates transmitted about the number of sEPSCs over gamma-cycle time windows (non-rhythmic, 0.43 ± 0.05 bits; gamma, 0.62 ± 0.04 bits; $P < 0.001$) and on longer timescales (theta-cycle time window: non-rhythmic, 1.17 ± 0.07 bits; gamma, 1.37 ± 0.04 bits; $P < 0.001$). In contrast, theta modulation increased sEPSC spike rate information only on theta-cycle timescales and longer (Fig. 2e). Similar results were obtained from both frontal (above) and prefrontal ($n = 5$ cells) layer V/VI pyramidal neurons,

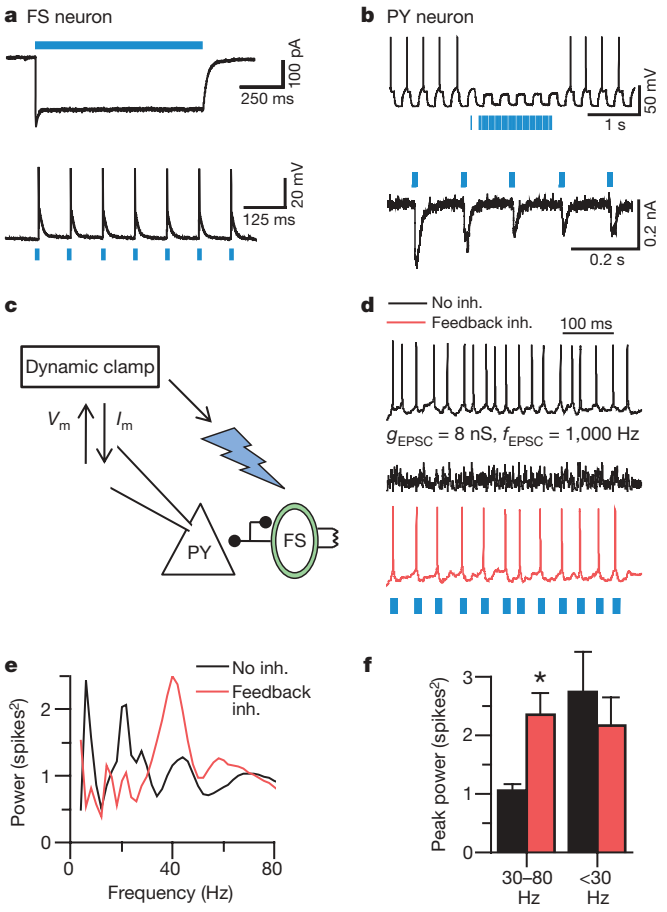

Figure 2 | Feedback inhibition from PV cells generates emergent gamma frequency synchrony. **a**, Light-evoked responses in a fast-spiking PV interneuron (FS). **b**, Responses of a ChR2(−) PY cell during photoactivation of ChR2(+) PV interneurons. **c**, Experimental design: sEPSCs drive PY cells. Light flashes triggered by PY cell spikes activate FS/PV interneurons (optical feedback inhibition). V_m, measured membrane potential; I_m, injected current. **d**, PY cell responses to non-rhythmic sEPSCs with and without this optical feedback inhibition (inh.). g_{EPSC}, unitary sEPSC conductance; f_{EPSC}, sEPSC frequency. **e**, Power spectra obtained by convolving the spike trains of a PY cell with wavelets of varying frequencies; red trace represents optical feedback inhibition via PV interneurons. **f**, Summary of spectral data at gamma (30–80 Hz) and lower frequencies ($n = 4$ cells; $^*P < 0.05$). Error bars, mean and s.e.m.

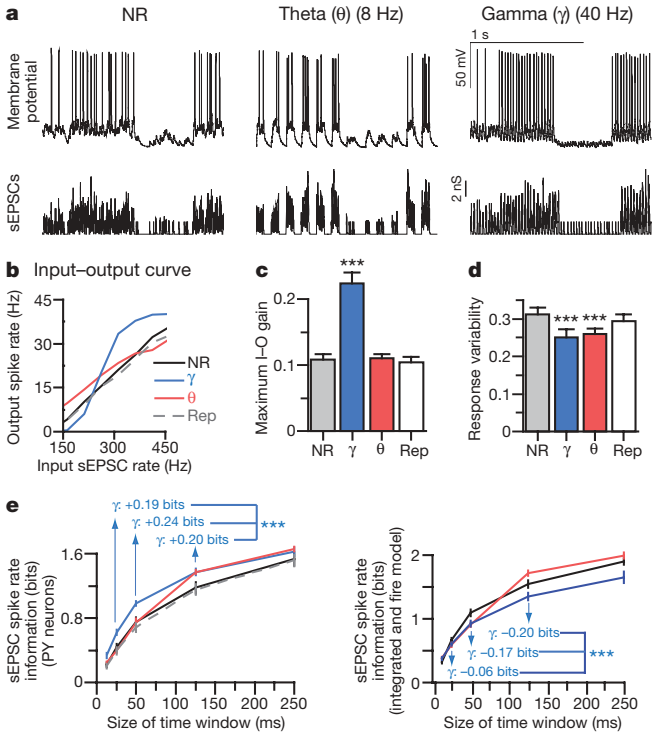

Figure 3 | Gamma oscillations amplify signals and reduce noise in PY cells. **a**, PY cell responses (top traces) to non-rhythmic (NR), repeated non-rhythmic (Rep), or rhythmic defined sEPSC trains (lower traces; Supplementary Information; depicted rates = 40–372 Hz). **b**, Spike rates of representative PY cell under each rhythmicity condition. **c**, Maximum input–output (I–O) gain. **d**, Response variability for each condition. **e**, Left: mutual information between output spike number and input sEPSCs; gamma oscillations consistently enhanced mutual information. Right: contrasting effect on sEPSC spike rate information in simulated integrate-and-fire cells using the same sEPSC trains ($n = 14$ cells in **c**–**e**; $^{***}P < 0.001$). Key in **e** is the same as for **b**. Error bars, mean and s.e.m.

and findings were robust to altering both sEPSC amplitudes and extents of oscillatory modulation (Supplementary Fig. 2). Information transmission changes could be accounted for entirely by decreased noise entropy (Supplementary Information; no increase in response entropy was observed), and this informational response to gamma-modulated input was not simply an effect of temporal summation, because simulated integrate-and-fire neurons receiving identical sEPSC trains did not enhance sEPSC spike rate information in response to gamma oscillations (Fig. 3e); instead, informational effects probably depend on specialized active conductances influencing native PY cells, as illustrated by biophysical models (Supplementary Fig. 8).

To extend these findings to trains of real EPSCs in large networks of neurons, we stimulated distributed populations of PY neurons in brain slices from transgenic mice expressing ChR2 under the *Thy1* promoter[21–23]. Specific expression in layer V pyramidal neurons and their processes (Fig. 4a), absence of light-evoked responses outside of layer V and absence of short-latency axonal-type responses to light all confirm that ChR2 activation was specific to layer V PY neurons, which comprise an interconnected network[24] that may maintain prefrontal activity during working memory[25] and generate UP states of persistent network activity[26]. We recorded from multiple layer V cell types, and classified neurons on the basis of morphology, intrinsic membrane properties and light responses; in particular, we used the fast-spiking phenotype to identify PV interneurons[1,2], which did not express eYFP (Fig. 4a) and were not directly activated by light (Fig. 4c, e; Supplementary Information). We delivered rhythmic and non-rhythmic trains of stimulation to the spatially distributed PY circuit population by full-field light flashes via a ×40 objective rather than by dynamic clamp. This approach recruits a small distributed population of neurons (~20–50 PY neurons, Supplementary Information) in a manner that has been useful for studying temporal aspects of circuit function in other circuits such as the retina[27].

Modulating trains of light flashes using theta or gamma frequency patterns induced pronounced rhythmic firing at the corresponding frequencies (Fig. 4f) in PY neurons ($n = 12$), as expected. A valuable property of these virtually identical mice from the transgenic ChR2 line is that spike trains are remarkably similar in different pyramidal neurons from different slices (Fig. 4d). We took advantage of this fact (Supplementary Information) to compute the information that fast-spiking interneuron responses convey about the output of PY neurons. Both theta and gamma oscillations increased the amount of information transmitted from the PY neuron population to post-synaptic fast-spiking interneurons (Fig. 4g, h; gamma, $P < 0.001$; theta, $P < 0.05$; $n = 7$ cells), and once again we found that gamma oscillations enhanced information transmission across timescales (for example, over 125 ms: non-rhythmic, 1.02 ± 0.11 bits; gamma, 1.44 ± 0.15 bits; $P < 0.001$, $n = 7$ cells). We probed regular-spiking interneurons as well (regular-spiking here refers to non-fast-spiking

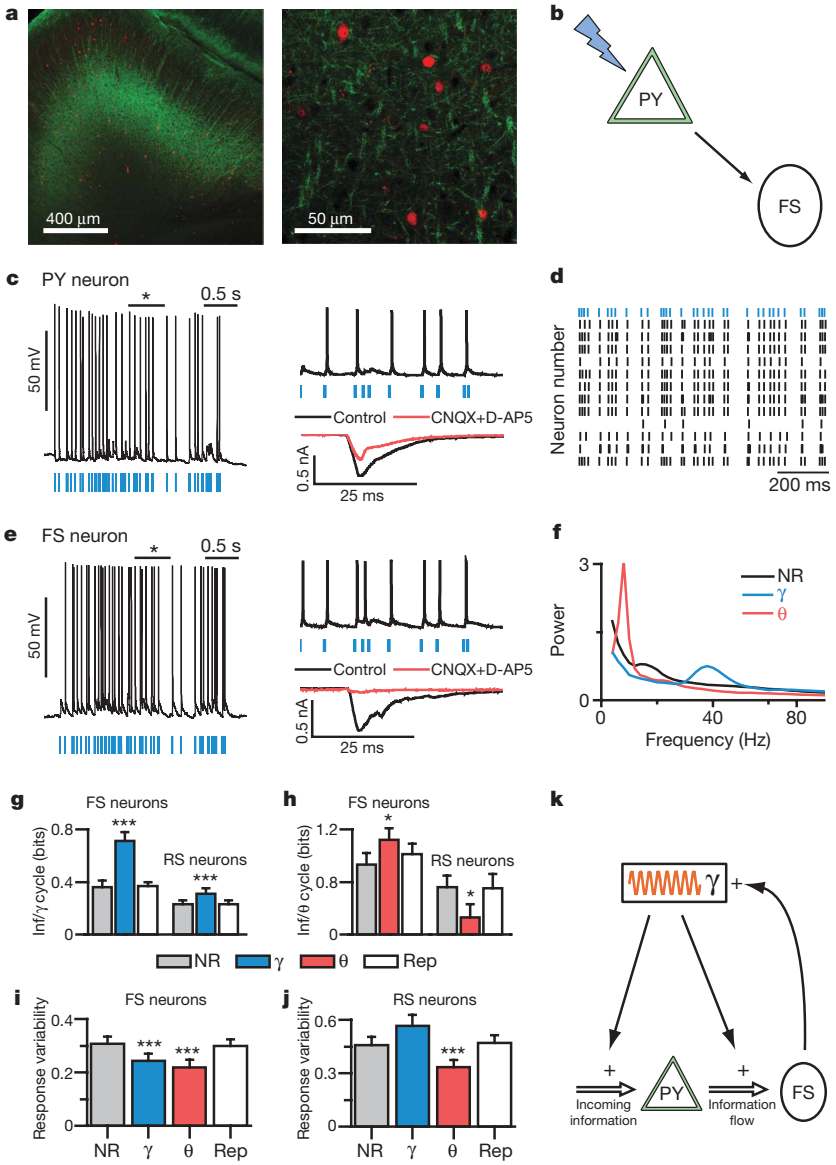

Figure 4 | Gamma oscillations enhance information flow from PY to PV cells. **a**, eYFP (green) and PV (red) cells in layer V PFC of *Thy1*−ChR2–eYFP transgenic mice. **b**, Experimental design: light flashes excite PY neurons, which synaptically excite PV cells. **c**, Light directly excites PY cells. Current evoked by 1-ms flashes with/without synaptic blockers (CNQX and D-AP5). **d**, Responses of PY neurons from different slices to the same light train (blue). **e**, Light indirectly excites fast-spiking (FS) interneurons. Current evoked by 1-ms flashes with/without synaptic blockers. **f**, Power spectra of PY neuron spiking elicited by distinct-rhythmicity light trains. **g**, **h**, Mutual information (Inf) between responses of fast-spiking or regular-spiking (RS) neurons and PY neurons to the same rhythmic or non-rhythmic light trains (Supplementary Information). **i**, **j**, Response variability of fast-spiking and regular-spiking cells for rhythmic and non-rhythmic stimuli ($n = 12$ PY, 7 fast-spiking, and 9 regular-spiking cells). **k**, Interplay of gamma (γ) oscillations and fast-spiking neurons. Error bars, mean and s.e.m.

neurons not directly activated by light; $n = 9$), and found surprising specificity of information effects to fast-spiking neurons; specifically, theta oscillations actually decreased information transmission through regular-spiking neurons (Fig. 4g, h, $P < 0.001$) and gamma oscillations exerted little effect on longer timescales (125 ms; $P = 0.82$, $n = 9$ cells). As in dynamic-clamp experiments (Fig. 3), oscillations reduced response variability (Fig. 4i, j, $P < 0.001$, $n = 7$ cells) and increased mutual information by decreasing noise entropy (noise entropies for 125-ms window: non-rhythmic, 1.73 ± 0.22 bits; gamma, 1.40 ± 0.26 bits; theta, 1.42 ± 0.22 bits; $P < 0.01$ and $P < 0.001$ for gamma and theta modulation, respectively; no increase in response entropy was observed). Decreases in noise entropy may relate to greater stereotypy in interspike intervals (ISIs) in PY neurons during rhythmic versus non-rhythmic states (Supplementary Fig. 3c). Indeed, by making ISIs more stereotyped, rhythmic modulation of inputs may reduce variability resulting from short-term plasticity and feedback inhibition, which are likely relevant to the effects of oscillations in neural circuits.

Pioneering work has suggested a role for fast-spiking PV interneurons in important aspects of information processing in the brain[7]. However, it has been unclear whether these interneurons are necessary or sufficient to promote gamma oscillations, and what causal role these oscillations would have in modulating information processing. Although further work will be needed to differentiate among different subtypes of PV interneurons—for example, basket and axo-axonic cells, which may have different functions[28]—we observed and quantified significant functional synergy between fast-spiking PV interneurons and gamma oscillations (Fig. 4k) in promoting transmission of signals within neocortical microcircuits. Through these mechanisms, gamma oscillations generated by fast-spiking PV interneurons could amplify signals corresponding to attended stimuli[29] and facilitate the transfer of information both within and between brain regions[30], while

corresponding abnormalities in this process may contribute to the disabling symptoms of schizophrenia[10] and autism[11]. The triad of optogenetics, dynamic clamp and informational analysis enables precise control over input data integrated with precise tracking and measurement of relevant output data. Simultaneous control over these input and output data streams may enable a novel kind of reverse engineering of microcircuits in both health and disease, by facilitating quantitative insight into how interacting elements give rise to normal and pathological circuit function.

METHODS SUMMARY

Viral-mediated opsin expression. We used a double-floxed inverted open reading frame strategy (Fig. 1a and Supplementary Figs 1 and 4) with two nested pairs of incompatible lox sites. In Cre-expressing cells, *ChR2−eYFP* or *eNpHR−eYFP* is first reversibly flipped into the sense orientation via either pair of sites (Fig. 1b); this enables a second irreversible excision that prevents further inversion (Fig. 1b). Double-floxed reversed *ChR2–eYFP* or *eNpHR–eYFP* virus was injected stereotactically into infralimbic cortex of 5–6-week-old *PV*::*Cre* mice.

***In vivo* recording.** Simultaneous optical stimulation and electrical recording in infralimbic and prelimbic cortex of PV::Cre transgenic mice was carried out as described previously[6]. We recorded local field potentials in mice anesthetized with a ketamine/xylazine mixture, and calculated power spectra immediately after blue light flashes that were separated from other flashes by at least 25 ms.

***In vitro* electrophysiology.** Patch-clamp recordings in brain slices and dynamic clamp were carried out as described previously[5]. All recordings were at 32.5 ± 1 °C unless stated otherwise. We stimulated ChR2 in pyramidal neurons using flashes of light lasting 1 ms generated by a 300 W Xenon lamp and a GFP filter set delivered to the slice through a ×40 objective. We used 5-ms light flashes to stimulate ChR2 in fast-spiking interneurons. We stimulated eNpHR in PV interneurons *in vitro* using continuous yellow light generated analogously using a 593 nm filter set.

sEPSC and light pulse trains. Experiments were divided into 5- or 10-s long sweeps, which were subdivided into 500-ms segments, containing 0–250 sEPSCs. Rhythmic and non-rhythmic trains used the same sequence of sEPSC rates. For non-rhythmic trains, sEPSCs occurred randomly across each segment. Within rhythmic trains, sEPSCs occurred only during half of each 25 or 125 ms cycle. All summary plots, bar graphs and numerical values in the text are presented as mean ± s.e.m.

Received 20 February; accepted 20 March 2009.
Published online 26 April 2009.

1. Kawaguchi, Y. & Kubota, Y. Neurochemical features and synaptic connections of large physiologically-identified GABAergic cells in the rat frontal cortex. *Neuroscience* **85,** 677–701 (1998).
2. Toledo-Rodriguez, M. *et al.* Correlation maps allow neuronal electrical properties to be predicted from single-cell gene expression profiles in rat neocortex. *Cereb. Cortex* **14,** 1310–1327 (2004).
3. Freund, T. F. Interneuron diversity series: Rhythm and mood in perisomatic inhibition. *Trends Neurosci.* **26,** 489–495 (2003).
4. Whittington, M. A., Traub, R. D. & Jefferys, J. G. Synchronized oscillations in interneuron networks driven by metabotropic glutamate receptor activation. *Nature* **373,** 612–615 (1995).
5. Ylinen, A. *et al.* Intracellular correlates of hippocampal theta rhythm in identified pyramidal cells, granule cells, and basket cells. *Hippocampus* **5,** 78–90 (1995).
6. Tamas, G., Buhl, E. H., Lorincz, A. & Somogyi, P. Proximally targeted GABAergic synapses and gap junctions synchronize cortical interneurons. *Nature Neurosci.* **3,** 366–371 (2000).
7. Fuchs, E. C. *et al.* Recruitment of parvalbumin-positive interneurons determines hippocampal function and associated behavior. *Neuron* **53,** 591–604 (2007).
8. Konig, P., Engel, A. K. & Singer, W. Integrator or coincidence detector? The role of the cortical neuron revisited. *Trends Neurosci.* **19,** 130–137 (1996).
9. Womelsdorf, T. *et al.* Modulation of neuronal interactions through neuronal synchronization. *Science* **316,** 1609–1612 (2007).
10. Lewis, D. A., Hashimoto, T. & Volk, D. W. Cortical inhibitory neurons and schizophrenia. *Nature Rev. Neurosci.* **6,** 312–324 (2005).
11. Orekhova, E. V. *et al.* Excess of high frequency electroencephalogram oscillations in boys with autism. *Biol. Psychiatry* **62,** 1022–1029 (2007).
12. Boyden, E. S., Zhang, F., Bamberg, E., Nagel, G. & Deisseroth, K. Millisecond-timescale, genetically targeted optical control of neural activity. *Nature Neurosci.* **8,** 1263–1268 (2005).
13. Zhang, F. *et al.* Multimodal fast optical interrogation of neural circuitry. *Nature* **446,** 633–639 (2007).
14. Aravanis, A. M. *et al.* An optical neural interface: *in vivo* control of rodent motor cortex with integrated fiberoptic and optogenetic technology. *J. Neural Eng.* **4,** S143–S156 (2007).
15. Meyer, A. H., Katona, I., Blatow, M., Rozov, A. & Monyer, H. *In vivo* labeling of parvalbumin-positive interneurons and analysis of electrical coupling in identified neurons. *J. Neurosci.* **22,** 7055–7064 (2002).
16. Livet, J. *et al.* Transgenic strategies for combinatorial expression of fluorescent proteins in the nervous system. *Nature* **450,** 56–62 (2007).
17. Conde, F., Lund, J. S. & Lewis, D. A. The hierarchical development of monkey visual cortical regions as revealed by the maturation of parvalbumin-immunoreactive neurons. *Brain Res.* **96,** 261–276 (1996).
18. Raghavachari, S. *et al.* Gating of human theta oscillations by a working memory task. *J. Neurosci.* **21,** 3175–3183 (2001).
19. Howard, M. W. *et al.* Gamma oscillations correlate with working memory load in humans. *Cereb. Cortex* **13,** 1369–1374 (2003).
20. de Ruyter van Steveninck, R. R., Lewen, G. D., Strong, S. P., Koberle, R. & Bialek, W. Reproducibility and variability in neural spike trains. *Science* **275,** 1805–1808 (1997).
21. Arenkiel, B. R. *et al. In vivo* light-induced activation of neural circuitry in transgenic mice expressing channelrhodopsin-2. *Neuron* **54,** 205–218 (2007).
22. Wang, H. *et al.* High-speed mapping of synaptic connectivity using photostimulation in Channelrhodopsin-2 transgenic mice. *Proc. Natl Acad. Sci. USA* **104,** 8143–8148 (2007).
23. Gradinaru, V. *et al.* Targeting and readout strategies for fast optical neural control *in vitro* and *in vivo*. *J. Neurosci.* **27,** 14231 (2007).
24. Bannister, A. P. Inter- and intra-laminar connections of pyramidal cells in the neocortex. *Neurosci. Res.* **53,** 95–103 (2005).
25. Sanchez-Vives, M. V. & McCormick, D. A. Cellular and network mechanisms of rhythmic recurrent activity in neocortex. *Nature Neurosci.* **3,** 1027–1034 (2000).
26. Luczak, A., Bartho, P., Marguet, S. L., Buzsaki, G. & Harris, K. D. Sequential structure of neocortical spontaneous activity *in vivo*. *Proc. Natl Acad. Sci. USA* **104,** 347–352 (2007).
27. Baccus, S. A. & Meister, M. Fast and slow contrast adaptation in retinal circuitry. *Neuron* **36,** 909–919 (2002).
28. Szabadics, J. *et al.* Excitatory effect of GABAergic axo-axonic cells in cortical microcircuits. *Science* **311,** 233–235 (2006).
29. Fries, P., Reynolds, J. H., Rorie, A. E. & Desimone, R. Modulation of oscillatory neuronal synchronization by selective visual attention. *Science* **291,** 1560–1563 (2001).
30. Rodriguez, E. *et al.* Perception's shadow: long-distance synchronization of human brain activity. *Nature* **397,** 430–433 (1999).

Supplementary Information is linked to the online version of the paper at www.nature.com/nature.

Acknowledgements We thank S. Arber for her gift of the PV::Cre mice, and we acknowledge the advice and suggestions of R. C. Malenka, J. Huguenard and S. Baccus on this work. All materials are freely distributed and supported by the Deisseroth laboratory (http://www.optogenetics.org). K.D. is supported by the President and Provost of Stanford University, BioX, Bioengineering, and by NIMH, NIDA, CIRM, NSF, and the Keck, McKnight and Coulter Foundations. F.Z. is supported by NINDS, and V.S.S. is supported by a T32 postdoctoral research training fellowship from NIMH.

Author Information Reprints and permissions information is available at www.nature.com/reprints. Correspondence and requests for materials should be addressed to K.D. (deissero@stanford.edu).